Tim-3 aggravates podocyte injury in diabetic nephropathy by promoting macrophage activation via the NF-κB/TNF-α pathway

Huimin Yang [1,2], Tingting Xie [2], Dengren Li [2], Xianhong Du [1], Tixiao Wang [1], Chunyang Li [1], Xiaojia Song [1], Leiqi Xu [4], Fan Yi [3], Xiaohong Liang [1], Lifen Gao [1], Xiangdong Yang [2,**], Chunhong Ma [1,*]

ABSTRACT

Objective: Macrophage-mediated inflammation plays a significant role in the development and progression of diabetic nephropathy (DN). However, the underlying mechanisms remain unclear. Studies suggest that T cell immunoglobulin domain and mucin domain-3 (Tim-3) has complicated roles in regulating macrophage activation, but its roles in the progression of DN are still completely unknown.

Methods: We downregulated Tim-3 expression in kidney (intrarenal injection of Tim-3 shRNA expressing lentivirus or global Tim-3 knockout mice) and induced DN by streptozotocin (STZ). We analyzed the degree of renal injury, especially the podocyte injury induced by activated macrophages *in vitro* and *in vivo*. Then, we transferred different bone marrow derived macrophages (BMs) into STZ-induced Tim-3 knockdown mice to examine the effects of Tim-3 on macrophages in DN.

Results: First, we found that Tim-3 expression on renal macrophages was increased in patients with DN and in two diabetic mouse models, i.e. STZ-induced diabetic mice and db/db mice, and positively correlated with renal dysfunction of DN patients. Tim-3 deficiency ameliorated renal damage in STZ-induced diabetes with concurrent increase in protein levels of Nephrin and WT-1. Similar effects were observed in mice with Tim-3 knockdown diabetic mice. Second, adoptive transfer of Tim-3-expressing macrophages, but not Tim-3 knockout macrophages, accelerated diabetic renal injury in DN mice, suggesting a key role for Tim-3 on macrophages in the development of DN. Furthermore, we found NF-κB activation and TNF-α excretion were upregulated by Tim-3 in diabetic kidneys, and podocyte injury was associated with the Tim-3-mediated activation of the NF-κB/TNF-α signaling pathway in DN macrophages both *in vivo and in vitro*.

Conclusions: These results suggest that Tim-3 functions as a key regulator in renal inflammatory processes and serves as a potential therapeutic target for renal injury in DN.

© 2019 The Authors. Published by Elsevier GmbH. This is an open access article under the CC BY-NC-ND license (http://creativecommons.org/licenses/by-nc-nd/4.0/).

Keywords Diabetic nephropathy; Tim-3; Macrophage; NF-κB; TNF-α

1. INTRODUCTION

Diabetic nephropathy (DN), characterized as glomerular hypertrophy with thickened basement membrane and increased extracellular matrix protein deposition, is the most common microvascular complication of diabetes mellitus (DM) [1]. In China, approximately 11% of the population suffer from diabetes [1], of which 30%—40% further progressed to DN [2], making it one of the most common causes of end-stage renal disease both in China and worldwide [2,3]. The etiology of DN is multifactorial and remains largely obscure, with hyperglycemia, advanced glycation end products (AGE) and oxidative stress as the leading factors, infiltrated immune cells and chronic inflammation in kidneys seem to be the common pathological consequences [4,5].

Monocytes/macrophages present the most abundant infiltrating immune cells in the kidney of DN [6], and the accumulation of macrophages mostly predicts renal function decline in DN patients [7]. It has been reported that macrophage depletion in kidney reduces albuminuria and halts renal inflammation and progression of DN [8]. Besides, some clinical trials show that effective receptor antagonists targeting pro-inflammatory macrophages could reduce renal injury and proteinuria in patients with DN [9]. NF-κB, one of the most important transcription factors in macrophages, can be activated by several cytokines, which in turn induces the production of pro-inflammatory mediators such as TNF-α, resulting in diabetic renal damage [10]. Treatment of diabetic rats with NF-κB inhibitors for 4 weeks led to reduced renal macrophage infiltration, decreased production of

[1]Key Laboratory for Experimental Teratology of Ministry of Education and Department of Immunology, Shandong University School of Basic Medical Science, Jinan, PR China [2]Department of Nephropathy, Qilu Hospital of Shandong University, Jinan, Shandong, PR China [3]Department of Pharmacology, Shandong University School of Basic Medical Science, Jinan, PR China [4]Department of Gastroenterology, Qilu Hospital of Shandong University, Jinan, Shandong, PR China

*Corresponding author. Key Laboratory for Experimental Teratology of Ministry of Education and Department of Immunology, Shandong University School of Basic Medical Science, No. 44 Wenhua West Road, Jinan, Shandong, 250012, PR China. Fax: +86 531 88382038. E-mail: machunhong@sdu.edu.cn (C. Ma).

**Corresponding author. Department of Nephropathy, Qilu Hospital of Shandong University, No. 107 Wenhua West Road, Jinan, Shandong, 250012, PR China. E-mail: yxd683@163.com (X. Yang).

inflammatory cytokines, and consequently reversed renal dysfunction [11]. Although NF-κB inhibitors are not currently used in the treatment of renal diseases, many drugs applied in clinical have been shown to suppress NF-κB signaling and decrease proteinuria [12,13]. Therefore, it is necessary to explore new factors that might be responsible for regulating renal inflammation, especially the NF-κB signaling pathway in renal macrophages, which may provide novel therapies to treat renal inflammation in the development of DN.

T cell immunoglobulin domain and mucin domain-3 (Tim-3), initially identified as a negative regulator of Th1 immunity, plays critical roles in various inflammatory diseases including tumor and chronic viral infection [14—16]. Previous studies show that Tim-3 is expressed on innate immune cells such as natural killer cells (NK), NKT cells, dendritic cells (DC), and macrophages, in which Tim-3 plays diverse regulatory roles [16]. However, in contrast to its well-recognized, negative regulation effects on T cell-immunity, the role of Tim-3 on macrophages is complex and controversial depending on distinct microenvironments [17]. Growing evidence demonstrated that Tim-3 on macrophages could balance the activation between M1 and M2 macrophages, acting as a pro-inflammatory or anti-inflammatory regulatory factor in diverse diseases [18,19]. On the one hand, Tim-3 reduces the release of pro-inflammatory cytokines, such as IFN-γ and IL-12 in dextran sulfate sodium (DSS)-induced inflammatory bowel disease (IBD) and ameliorates the colitis [20]. However, on the other hand, Tim-3 highly expressed in hypoxic brain regions of cerebral hypoxia-ischaemia (H/I) linked the inflammation and subsequent brain damage to a hypoxia-inducible factor (HIF)-1-dependent way [21]. This is also consistent with another study about intracerebral hemorrhage (ICH) [18]. Our previous study demonstrated that Tim-3 inhibited hepatic inflammation via downregulation of ROS and NLRP3 inflammasome activation in nonalcoholic fatty liver disease (NAFLD), suggesting a protective role in chronic inflammatory diseases [22].

DN is one of the most common chronic kidney diseases (CDK) with macrophage infiltration [5], in which NF-κB, also known as p65, acts as a key mediator. Tim-3 is originally reported to inhibit NF-κB signaling by increasing PI3K-AKT phosphorylation and A20 expression and relives LPS-induced sepsis in mice [23]. However, the opposite function is also found that Tim-3 could activate NF-κB signaling in macrophages [24,25]. Till now, the roles of Tim-3 regulated NF-κB signaling in renal macrophages and in macrophage-mediated renal injury are completely unknown. In this study, our goal is to investigate Tim-3 function via the NF-κB/TNF-α signaling pathway in macrophages *in vitro* and *in vivo* assays of DN progression.

2. MATERIALS AND METHODS

2.1. Human renal biopsy samples
Samples from patients who had been diagnosed with diabetic nephropathy through renal biopsies were collected from the Department of Pathology, Qilu Hospital affiliated to Shandong Univeristy. Control samples were obtained from healthy kidney poles of individuals who underwent tumor nephrectomies without diabetes or renal diseases. The investigations were conducted in accordance with the Research Ethics Committee of Shandong University after informing the patients.

2.2. Animal experiments
Wild-type male C57BL/6 mice were purchased from Shandong University Experimental Animal Center (Jinan, China). Tim-3 TALEN (Tim-3KO) mice were generated by SiDanSai Biotechnology Company (Shanghai, China) [26], and db/db mice were obtained from the Jackson laboratory (Nevada, USA). During the experiments, all mice

were housed in a controlled environment with unrestricted access to food and water in accordance with the Institutional Animal Care and Use Committee procedures of Shandong University.

Mice underwent unilateral nephrectomy (Unx) with intrarenal delivery with shTim-3-lv or ctrl-lv (2×10^6 IU/kidney) to the intact kidney [27,28]. The detailed procedure is presented in the Supplementary Materials and Methods. After one-week recovery from unilateral nephrectomy, mice rendered diabetic were induced by intraperitoneal (I.P) injection of STZ (S0130, Sigma, St. Louis, MO, USA) at a dose 50 mg per kg body weight in sodium citrate buffer as previously described [29].

2.3. Renal macrophage isolation
Renal macrophages were isolated from kidney of sacrificed mice and pre-incubated with medium containing collagenase I or IV (100 mg/kidney) for 60 min in a 37 °C water bath. After lysing red blood cells (RBCs) and filtering the cells, cells were separated by 40% Percoll density gradient centrifugation. Cells were resuspended in 0.1 mM PBS buffer and subjected to flow cytometry [30].

2.4. Flow cytometry
The isolated immune cells were resuspended in 0.1 mM PBS and passed through a 70-μm strainer (BD Biosciences, NJ,USA). Samples were analyzed with the following antibodies: anti-human CD14 FITC (325604, Biolegend, San Diego, CA, USA); anti-human Tim-3 PE (345006, Biolegend, San Diego, CA, USA); anti-mouse CD45 APC-eFlour780 (47-0451-82, eBioscience, San Diego, CA, USA), anti-mouse F4/80 PE-eFlour610 (61-4801-82, eBioscience, San Diego, CA, USA); anti-mouse CD11b PE-Cy7 (25-0112-82, eBioscience, San Diego, CA, USA), CD3 APC (100236, Biolegend, San Diego, CA, USA), CD4 percycy5.5 (103132, Biolegend, San Diego, CA, USA), CD8 FITC (100706, Biolegend, San Diego, CA, USA), CD11c APC (17-0114-81, eBioscience, San Diego, CA, USA), NK1.1 pecy7 (25-5941-82, eBioscience, San Diego, CA, USA), anti-mouse Tim-3 PE (12-5870-82, eBioscience, San Diego, CA, USA). Antibodies and their isotype-matched negative control antibodies were incubated with cells at 4 °C for 30 min in dark. Cells were washed with 0.1 mM PBS. The samples were subjected and detected by a Beckman CytoFLEX FCM, and the data were analyzed by CytExpert 2.0 software.

2.5. Cell culture and treatments

2.5.1. Peritoneal macrophage isolation
Mice were intraperitoneally injected with 6% sterile starch solution at the dose of 1 ml per mouse. After 48—72 h, mice were sacrificed, and peritoneal macrophages (PMs) were obtained by injecting 5 ml of 0.1M PBS into the peritoneal cavity, massaging the cavity and withdrawing the fluid. The fluid was centrifuged at 1000 rpm for 5 min, and PMs were resuspended in RPMI-1640 medium with normal glucose (11 mol/l) (SH30809.01B, Thermo Fisher, Massachusetts), containing 10% fetal bovine serum (FBS), 100 U/ml Penicillin & Streptomycin (PS). PMs were incubated at 37 °C in 5% CO_2 for 3 h to allow macrophages to adhere. Non adherent cells were washed and removed with PBS buffer.

2.5.2. Bone marrow derived macrophage isolation
Bone marrow cells (BMs) were isolated from femur and tibia of mice under sterile conditions. The BMs were cultured in RPMI-1640 medium with normal glucose (11 mol/l), plus 10% FBS, 100 U/ml PS, 10 ng/ml macrophage colony stimulating factor (M-CSF) (NOVUS, Colorado, NBP-35165, USA) for 5—7 days to induce macrophage differentiation.

2.5.3. Podocyte cell lines

Conditionally immortalized mouse podocytes (MPC5) were obtained from Dr. Peter Mundel (Mount Sinai School of Medicine, New York, USA). MPC were cultured in RPMI-1640 medium at 33 °C and 5% CO_2. After differentiation at 37 °C for 10—14 d without interferon-γ, the podocytes were used for the following experiments. The MPC were cultured with macrophages conditioned medium containing different concentration of glucose and advanced glycation end products.

2.6. Co-culture podocytes with macrophages

2.6.1. Conditioned medium (CM) stimulation

In the CM stimulated experiments, PMs (1×10^6cells/ml) from WT or Tim-3KO mice were planted on six well plates and stimulated with NG or HG medium for 24h-48. MPC (4×10^5cells/ml) were planted on six well plates and cultured overnight in NG RPMI 1640 medium. Then, NG-CM or HG-CM from different PMs was added to podocytes for 24 h. Different stimuli were used in this study: (1) Normal glucose (NG, 11 mmol/L); (2) High glucose medium (HG, 20 and 40 mmol/L); (3) Mannitol (MA, 40 mmol/L) (3) Advanced glycation end product (AGE, 50—200 μg/ml); (4) Bovine serum albumin (200 μg/ml).

2.6.2. Transwell migration assay

In a transwell co-culture system, MPC (5×10^4) (upper) were seeded on a 0.8 μm transwell insert (Corning, NY, USA) with medium without FBS and co-cultured with PMs (1×10^6) (lower) from WT or KO mice in the absence or presence of HG treatment for 12 h. Imaged were captured with an Olympus optical microscope (IX73, Olympus, Tokyo, Japan).
The final analysis of the images was performed using Image J software.

2.6.3. Scratch assay

Podocytes were seeded on twelve-well plates. Each well was scratched with a sterile 10 μl pipette tip and incubated with macrophage CM including WT-NG, KO-NG, WT-HG, and WT-HG. The migration of podocytes in each stimulation group was observed after 12 h incubation. Podocytes were photographed 12 h after scratching with microscopy, and the number of cells that migrated into the scratched area was counted by Image Pro Plus6.0 software.

2.7. Si-RNAs transfection and inhibitors

RNA interference mediated by si-RNA was performed in PMs for 48 h. The specific si-RNA against Tim-3 was synthesized by GenePharma company in Shanghai, China.
Havcr2-mus-307 (sense: 5′- CCAGCAGAUACCAGCUAAAUU-3′, anti-sense:5′-UUUAGCUGGUAUCUGCUGGUU-3′) and a scrambled control si-RNA (sense: 5′-UUCUCCGAACGUGUCACGUUU′, anti-sense: 5′-ACGU-GACACGUUCGGAGAAUU-3′). Si-RNA transfection was carried out with lipofectamine (11668019, Invitrogen, Carlsbad, CA, United States) according to the procedure recommended by the manufacturer.
NF-κB inhibitor: BAY 11-7821 (B5556, Sigma, St. Louis, MO, USA) is a selective and irreversible inhibitor of IκB-α phosphorylation. BAY (10 μM) or DMSO (10 μM) control was added to cells pretreated for 1 h before NG or HG was added to macrophages.

2.8. Adoptive transfer of BMs into DN mice

The shTim-3-lv was delivered into renal tissue to knock down the expression of Tim-3 in kidney as previously described in STZ diabetic mice. BMs were collected from WT mice and Tim-3KO mice and adoptively transferred (2×10^6 cells) into STZ-treated diabetic mice through tail vein injection once a month. Wild-type mice received BM transfer (BMT) obtained from GFP transgenic mice. The mice were sacrificed one month after the BMT and FCM was used to evaluate the efficiency of BMT [31].

2.9. RNA extraction and real-time PCR analysis

Total RNA were extracted from renal cortical tissue or cultured cells with Trizol (15596-018, Invitrogen, Carlsbad, CA, United States) and reversed transcribed into cDNA. Real-time PCR was performed using SYBR Green reagent on the ABI 7500 Real-time PCR System (Applied Biosystems, Carlsbad, CA, USA). The following primers were used for mRNA detection:
mβ-actin forward 5′-TGCGTGACATCAAAGAGAAG-3′, reverse 5′-TCCATACCCAAGAAGGAAGG-3′; mTim-3 forward 5′-CTCCAA-GAACCCTAACCACG-3′, reverse 5′-AGCCCATGTGGAAATTTTTG-3′; mTNF-α forward 5′-CAGCCTCTTCTCATTCCTGC-3′, reverse 5′-GGTCTGGGCCATAGAACTGA-3′; mIL-6 forward 5′- GATGGATGCTAC-CAAACTGGA-3′, reverse 5′-TCTGAAGGACTCTGGCTTTG-3′; mPodocin forward 5′- TGAGGATGGCGGCTGAGAT-3′, reverse 5′-GGTTTGGAG-GAAVTTGGGT-3′; mCD2AP forward 5′- GGAATTCAGCCACATCCACAA-3′, reverse5′-ACGATCAATTCCAGTTCGTCCTC-3′;
The relative gene expression was determined after normalization.

2.10. Western blot analysis

Kidney and cell lysates were extracted with extraction buffer (RIPA), and 30 μg of protein extract was prepared for use. The samples were separated by sodium dodecyl sulfate polyacrylamide gel electrophoresis (SDS-PAGE) and then transferred into a PVDF membrane and incubated with primary antibody in 5% milk or BSA to block other contaminants. Antibodies used in this study are summarized as follows: anti-β-actin antibody (60008-1-Ig, 1:5000, Proteintech, Wuhan, China), anti-Tim-3 (ab185703, 1:800, Abcam, Southampton, UK), anti-Nephrin (BA1669, 1:1000, Boster, Wuhan, China), anti-P65 NF-κB antibody (8242S, 1:1000, CST, MA, USA), anti-phosphorylated P65 NF-κB antibody (3033S, 1:1000, CST, MA, USA), anti-caspase-3 (9665S, 1:1000, CST, MA, USA).

2.11. Immunohistochemistry staining assay

For immunostaining of macrophages and podocytes, 3 μm thick formalin fixed, paraffin embedded kidney sections were stained with anti-Tim-3 antibody (ab185703, 1:200, Abcam, Southampton, UK), anti-Tim-3 (60355-1-Ig, 1:200, Proteintech, Wuhan, China), anti-CD68 antibody (ab955, 1:100, Abcam, Southampton, UK), anti-Nephrin antibody (ab136894, 1:200, Abcam, Southampton, UK), anti-WT-1 antibody (ab212951, 1:500, Abcam, Southampton, UK), anti-phosphorylated P65 NF-κB antibody (3033S, 1:100, CST, MA, USA) as primary antibody and anti-mouse and anti-rabbit (PV-9000, 1:200, ZSBIO, Beijing, China) as secondary antibody. Images were captured using an optical microscope. The final analysis of the images was performed using the software Image Pro Plus6.0.

2.12. Immunofluorescence staining

For immunostaining of double-labeled Tim-3 on macrophages and Tim-3 with p-p65, 10 μm thick formalin fixed, frozen embedded kidney sections were stained with anti-Tim-3 (Rab) antibody/anti-CD68 antibody, anti-Tim-3 (mus) antibody/anti-p-p65 antibody as former described. Secondary antibodies (Alexa Fluor 488-conjugated goat anti-mouse, Alexa Fluor 647-conjugated goat anti-rabbit, Proteintech, Wuhan, China) were incubated for 30 min at 37 °C in the dark. Nucleus was labeled with DAPI, and images were detected with Olympus optical microscope. The actin cytoskeleton was stained with

primary anti-phalloidin-TRITC (40734ES75, 1:100, YESEN, Shanghai, China), and images were captured by confocal laser-scanning microscopy with a LSM780 laser scanning confocal microscope (Carl Zeiss, Oberkochen, Germany) at Shandong University. The final analysis of the overlay were performed using the software Zen2010.

2.13. Transmission electron microscopy (TEM)

The ultrastructure of podocyte foot process from diabetic mice was analyzed after sacrificed. The tissues were sliced into cubes ≤ 1 m^3 and were immersed into 2.5%, samples were handled and detected in Weiya subelectron microscope lab of Jinan, Shandong Province. The GBM thickness, foot process width and number of foot processes were calculated.

2.14. Statistics

Data are expressed as the means $\pm$ SEM. The Student's t-test was employed for comparisons between two groups, and one-way analysis of variance (ANOVA) followed by Tukey's post-test for multiple comparisons was used for groups of three or more. $P < 0.05$ was considered statistically significant. *In vitro* and *in vivo* experiments were assessed in at least three independent experiments. Differences were evaluated using GraphPad Prism. Statistical significance was set at a $P < 0.05$. *$P < 0.05$, **$P < 0.01$, ***$P < 0.001$, ****$P < 0.001$.

3. RESULTS

3.1. Augmented Tim-3 expression correlates with renal injury in DN

To investigate whether Tim-3 expression is associated with renal injury in DN, we measured protein and mRNA levels of Tim-3 in renal tissue from control mice, STZ-induced DN mice and diabetic db/db mice. Western blot and real-time PCR analyses showed that Tim-3 expression was increased in renal tissue of STZ-induced DN mice (Figure 1A, B) in a time-dependent manner (Supplementary Fig. S1A). A similar increase was also observed in db/db mice (Figure 1A, B). The renal damage in STZ and db/db mice was confirmed by enhanced urinary protein excretion (increased urinary albumin to creatinine ratio, UACR) (Supplementary Fig. S1B), aggravated mesangial matrix expansion and decreased levels of Nephrin and Wilms' tumor protein-1 (WT-1) in glomeruli (Figure 1C). Immunohistochemistry (IHC) staining and immunofluorescent (IF) staining confirmed the augmented expression of Tim-3 in renal tissue (Figure 1C and Supplementary Fig. S1C, D) with increased CD68$^+$ macrophages infiltration and decreased Nephrin and WT-1 expressions in renal tissue of DN mice (Figure 1C). Dual IF staining verified the co-localization of Tim-3 with CD68$^+$ macrophages in glomeruli and showed a higher degree of co-localization in STZ mice (Figure 1D). Furthermore, flow cytometry (FCM) analysis showed that renal infiltrating macrophages exhibiting F4/80^{low} CD11b^{high} markers were increased in diabetic kidneys, whereas the F4/80^{high} CD11b^{low} macrophages were decreased (Figure 1E). Tim-3 expression was selectively augmented on F4/80^{high} CD11b^{low} and F4/80^{low} CD11b^{high} subsets of renal macrophages but less expressed on other subsets of immune cells from DN mice (Figure 1E and Supplementary Fig. S1E). These results suggest that Tim-3 might be responsible for macrophage activation in DN. To determine whether the augmented Tim-3 expression is associated with renal injury in DN, both peripheral blood and renal biopsy samples from healthy control subjects and DN patients were used. As shown in Figure 2A, both the percentage of CD14$^+$ monocytes/macrophages and Tim-3 expression on CD14$^+$ monocytes/macrophages were significantly increased in patients with DN (n = 18) compared with

control subjects (n = 18). Moreover, IHC assays in consecutive renal tissue sections and dual IF assays displayed increased expression of Tim-3 and CD68$^+$ macrophages in kidneys of DN patients, and exhibited co-localization of Tim-3 and CD68$^+$ in renal macrophages (Figure 2B and Supplementary S2A). In addition, quantification of IHC staining demonstrated that the level of Tim-3 was negatively correlated with the estimated glomerular filtration rate (eGFR) (Spearman R^2 = 0.6415, $P < 0.01$, n = 14) (Figure 2C) but positively associated with UACR in DN patients (Spearman R^2 = 0.3437, $P < 0.05$, n = 14) (Figure 2D). Moreover, Tim-3 was found to be expressed in renal biopsies from different forms of nephropathy, indicating its potential involvement in different forms of chronic kidney diseases (CKD) (Supplementary Fig. S2C).

3.2. Reduction of Tim-3 ameliorates podocyte injury and proteinuria in DN mice

To elucidate the potential roles of Tim-3 in podocyte damage, Tim-3 shRNA-expressing lentivirus was used to induce tissue-specific knockdown (KD) and TALEN system was used to prepare global Tim-3 knockout mice [22]. Firstly, Tim-3 shRNA-expressing lentivirus was locally injected into the renal cortex of C57BL/6 mice, along with Unx and STZ treatment to generate diabetic Tim-3 KD mice. The efficient and sustained Tim-3 knockdown in kidney was confirmed by western blot and IHC staining (Supplementary Fig. S3A, B). In order to exclude the blood pressure variation after Unx, the blood pressure of diabetic rats was measured after two week of Unx. As shown in Supplementary Fig. S3C, rats BP demonstrated no statistical difference before or after Unx as previous reported [32,33]. As shown in Figure 3A,B, levels of UACR and ratio of kidney to body weight (KBWR) were reduced in diabetic Tim-3 KD mice compared with the control lentivirus (ctrl-lv)-treated group without significant changes in body weight rates and blood glucose levels (Supplementary Fig. S3D, E), indicating that Tim-3 KD relieved STZ-induced renal damage. Consistently, diabetic Tim-3 KD mice displayed decreased apoptosis of renal parenchymal cells (Figure 3C), reduced STZ-induced mesangial matrix expansion and upregulated of podocyte phenotypic markers Nephrin and WT-1 in renal tissue (Figure 3D,E). In line with these findings, transmission electron microscope (TEM) analysis showed that Tim-3 KD greatly alleviated STZ-induced glomerular basement membrane (GBM) thickness and maintained numbers of podocyte foot process (Figure 3F).
Consistent with the results obtained from Tim-3 KD mice, global Tim-3 KO diabetic mice demonstrated reduced UACR and KBWR levels (Figure 3G,H), decreased renal parenchyma cell apoptosis (Figure 3I), ameliorated mesangial matrix expansion, and attenuated podocyte effacement as evidenced by levels of Nephrin and WT-1 (Figure 3J and Supplementary Fig. S3F). Relatively reduced Tim-3 expression in renal tissue and renal macrophages was confirmed by western blot and FCM (Supplementary Fig. S3G, H). Together, these observations strongly suggest a critical role for Tim-3 in diabetic renal damage and confirm that Tim-3 induces renal inflammation and podocyte injury in DN mice.

3.3. Adoptive transfer of Tim-3-positive macrophages aggravates podocyte dysfunction

Tim-3 expression has been detected in different immune cells, among which macrophages are the most abundant subset infiltrated in renal tissue from DN individuals [4]. Our data from DN mice and DN patients clearly demonstrated enhanced Tim-3 expression on renal macrophages. To explore the role of Tim-3-mediated macrophage activation in DN, adoptive transfer of bone marrow-derived macrophages (BMs) were included to exclude the influence of Tim-3 expressed on other
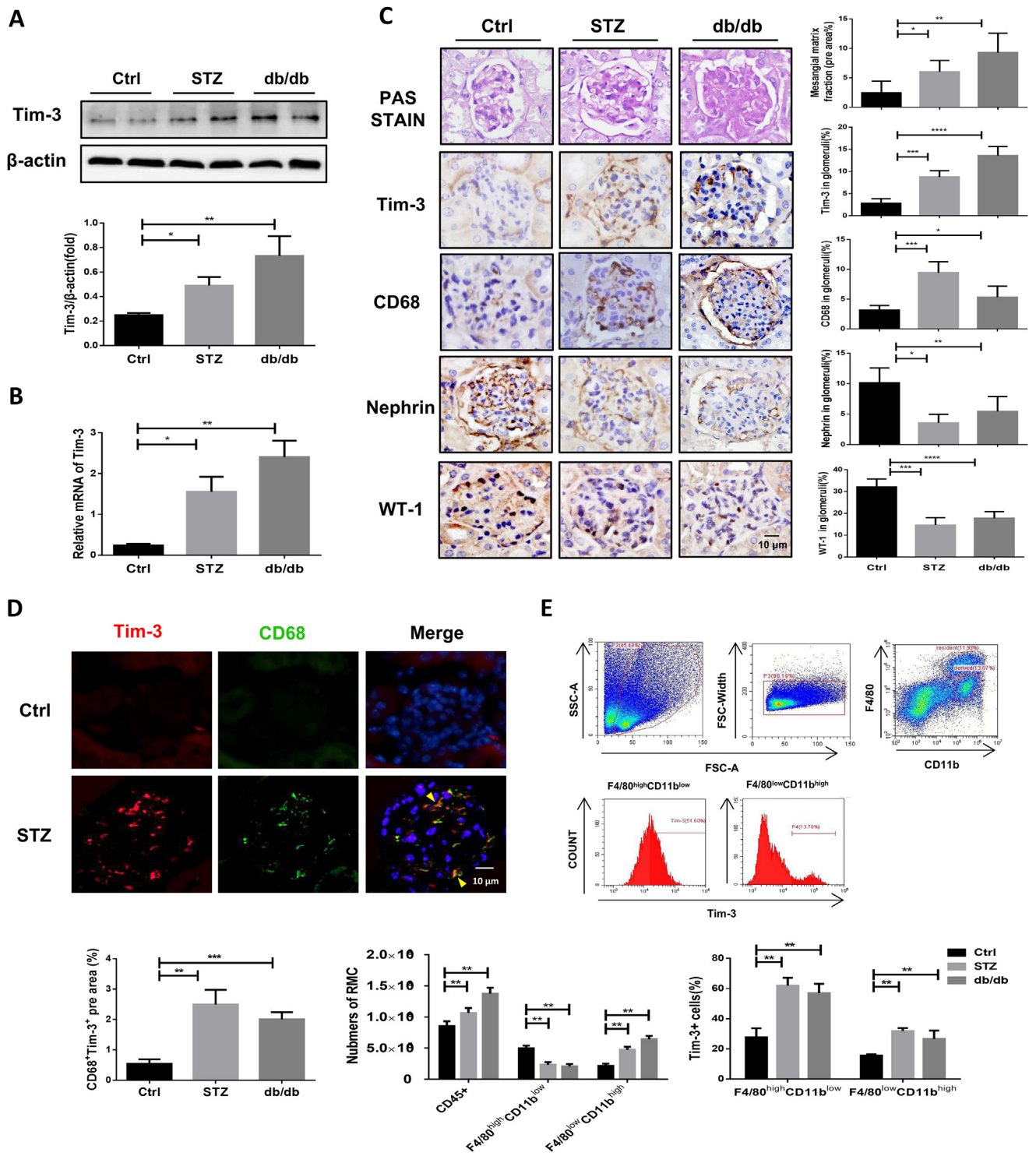
Figure 1: Tim-3 was increased in the renal macrophages of DN mice. Western blot (A) and RT-PCR (B) analyses showing the expressions of Tim-3 in kidneys from Ctrl, STZ and db/db mice. (C) Representative photomicrographs of Periodic Acid-Schiff (PAS) staining and immunohistochemical (IHC) staining of Tim-3, CD68, Nephrin, and WT-1 in renal glomeruli of different mice. (D) Representative photomicrographs of double-labeled immunofluorescence (IF) staining of Tim-3 (red), CD68 (green) and nucleus (blue) in renal glomeruli of STZ mice. Bar = 10 μm. (E) Representative flow cytometry (FCM) of Tim-3 expressions in renal macrophages of different mice. The bars represent the mean values and the stand, ad errors of the means (Mean ± SEM). *P < 0.05, **P < 0.01, ***P < 0.001 vs normal control.

cells. Briefly, bone marrow cells separated from WT and Tim-3 KO mice were stimulated with M-CSF and high glucose (HG) medium for 5 days, and the cells were transferred back into diabetic Tim-3 KD mice via tail vein injection once a month (Figure 4A). The presence of

transferred BMs in renal tissue was confirmed by FCM with renal macrophages from GFP-transgene mice (Supplementary Fig. S4A). In Supplementary Fig. S4B, the percentage of macrophages with/without transferring had no statistical difference, suggesting that this
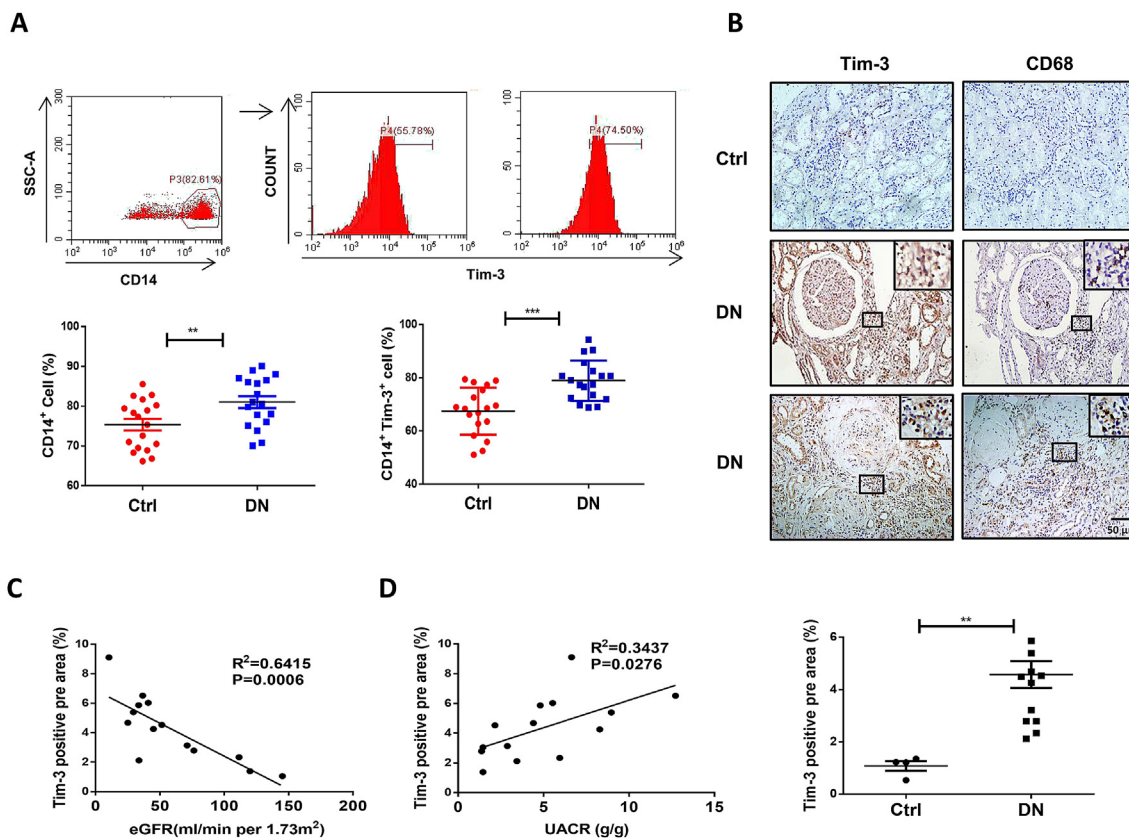
Figure 2: Upregulation of Tim-3 in renal biopsies of DN patients. (A) Representative FCM analysis showing the percentages of $CD14^+$ monocytes/macrophages and $Tim-3^+$ $CD14^+$ subpopulation from PBMC of DN patients and healthy controls. (B) Representative photomicrographs and quantification of Tim-3 IHC staining in human renal biopsies from DN patients (n = 14) and controls (n = 4). Bar = 50 μm. (C) Negative correlation between Tim-3 IHC staining levels and estimated glomerular filtration rate (eGFR) in DN patients (Spearman R^2 = 0.6415, P < 0.01). (D) Positive correlation between Tim-3 IHC staining levels and UACR in DN patients (Spearman R^2 = 0.3437, P < 0.05). PBMC, peripheral blood mononuclear cells (n = 18); Ctrl, healthy control; DN, diabetic nephropathy; Photographs were quantified with Image Pro Plus6.0 (IPP) software.

experiment reflects the physiologic conditions of mice. As expected, adoptive transfer of BMs from WT and Tim-3 KO mice had no effect on body weights and blood glucose levels during the period of DN (Supplementary Fig. S4C, D). However, macrophage transplantation with WT mice resulted in significantly increased levels of UACR, KBWR (Figure 4B, C) and a higher frequency of renal parenchyma cell apoptosis (Figure 4D) compared with that of the Tim-3 KO BMT group. Consistently, adoptive transfer of BMs from WT mice decreased the expression of Nephrin and WT-1, together with serious mesangial matrix expansion and glomerular hypertrophy (Figure 4E,F). Collectively, these data suggests that Tim-3-expressing macrophages promote renal injury in DN mice.

3.4. Tim-3 triggers podocyte injury by activating macrophages
Podocyte injury has been identified as a critical process resulting in proteinuric kidney disease, and podocytopenia mediated by hyperglycemia induced podocyte apoptosis are common in DN patients and in DN mice [34]. Although accumulated data suggest a critical role of hyperactivated macrophages in podocyte injury [35], the regulatory mechanisms linking macrophages to podocytes remain to be elucidated. To address this, the involvement of Tim-3 on macrophage-initiated podocyte injury was investigated in a model *in vitro*. Firstly, HG and AGE were used to stimulate peritoneal macrophages (PMs) and

BMs to mimic the local microenvironment in DN. In accordance with *in vivo* data, both HG and AGE significantly increased Tim-3 expression in PMs and BMs in a dose dependent manner (Figure 5A and Supplementary Fig. S5A—B), accompanied with elevated levels of pro-inflammatory cytokines, such as TNF-α, IL-6, and IL-1β (Supplementary Fig. S5B). Next, in order to demonstrate the role of Tim-3 in the interaction between macrophages and podocytes, conditioned medium (CM) prepared from NG/HG-stimulated macrophages from either WT or Tim-3 KO mice was used to treat cell line of mouse podocyte cells (MPC). Tim-3 deficiency on macrophages from Tim-3 KO mice was confirmed by western blot and RT-PCR (Supplementary Fig. S5C—D). As shown in Figure 5B,C, in agreement with previous report [35]. CM from HG-stimulated macrophages caused podocyte apoptosis and decreased Nephrin expression in MPC. However, this decrease was almost completely reversed by CM from Tim-3-deficient macrophages (KO-CM) (Figure 5B). The relative mRNA levels of Podocin and CD2AP, two podocyte structural and morphological markers, were significantly augmented in MPC treated with CM from Tim-3-deficient macrophages (Figure 5C). Moreover, confocal microscopy images showed that podocytes treated with CM from Tim-3 deficient macrophages displayed much thinner actin filaments and fewer non-fiber-like microfilament cytoskeleton (Figure 5D), suggesting an amelioration of actin cytoskeleton derangement in
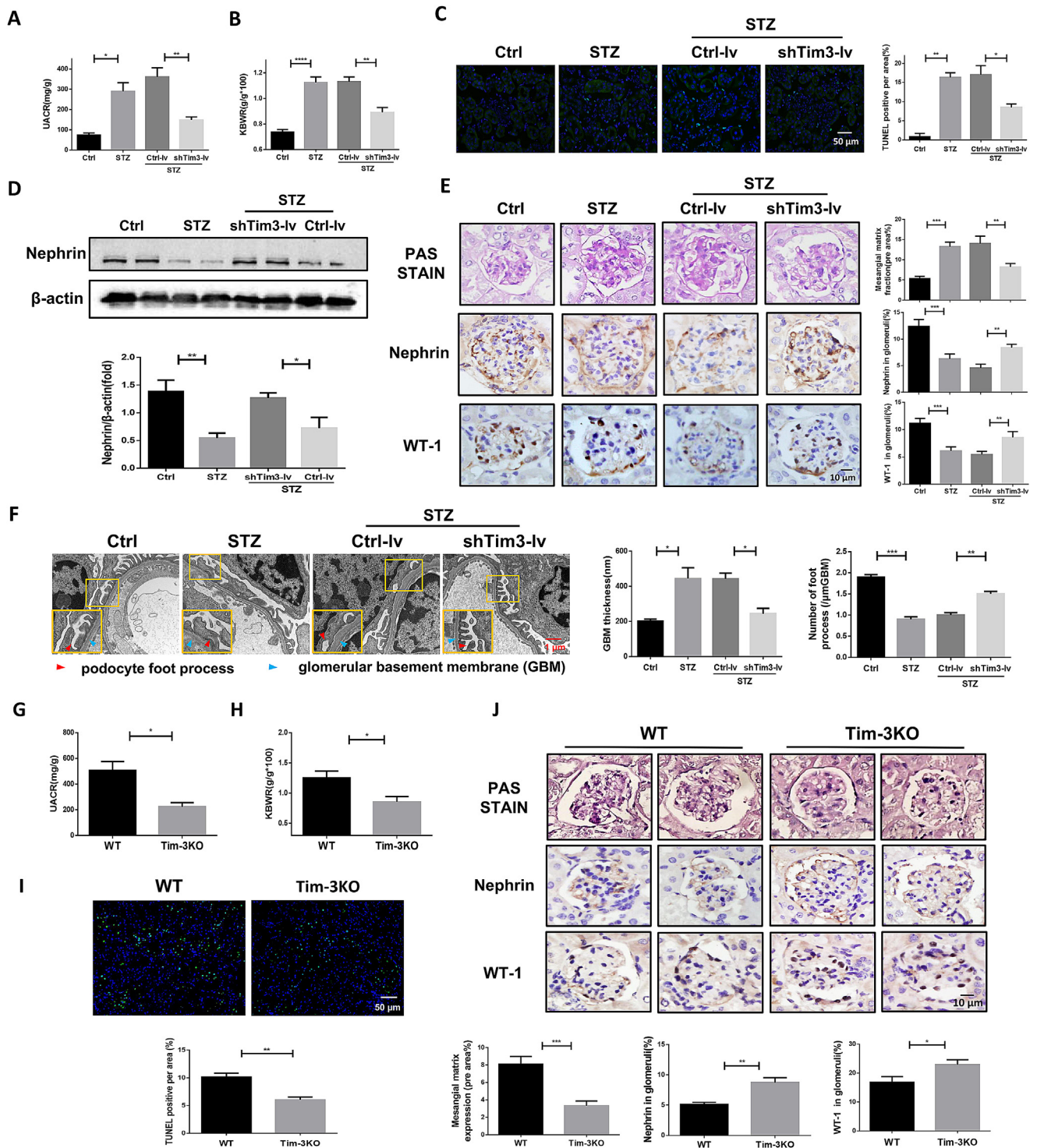
Figure 3: Reduction of Tim-3 ameliorated podocyte injury and proteinuria in DN mice. UACR (A) and the ratio of kidney weight to body weight (KBWR) (B) in Tim-3 KD mice at 16 weeks of age after STZ injection. (C) Representative photomicrographs of TUNEL staining for apoptotic cells in the different groups. Bars = 50 μm. (D) Representative western blot analysis showing the relative protein levels of Tim-3 and Nephrin in renal tissue of the different groups. (E) Representative photomicrographs and quantifications of PAS staining and IHC staining of Nephrin and WT-1 in renal tissue of the different groups. Bars = 10 μm. (F) Representative transmission electron micrographs and quantifications of glomerular basement membrane (GBM) thickness and numbers of podocyte foot processes in the glomeruli of different groups. Bars = 2 μm; 1 μm. UACR (G) and KBWR (H) levels from WT and Tim-3 KO mice at 12 weeks of age after STZ injection. (I) Representative photomicrographs of TUNEL staining for apoptotic cells in the different groups. Bars = 50 μm. (J) Representative photomicrographs and quantifications of PAS staining and IHC staining of Nephrin and WT-1 in renal tissue of the different groups. Bars = 10 μm *P < 0.05, **P < 0.01, ***P < 0.001. Tim-3 KD mice, shTim-3-lv knockdown diabetic mice (n = 6); Tim-3 KO mice, Tim-3 talen-target knockout diabetic mice (n = 3).
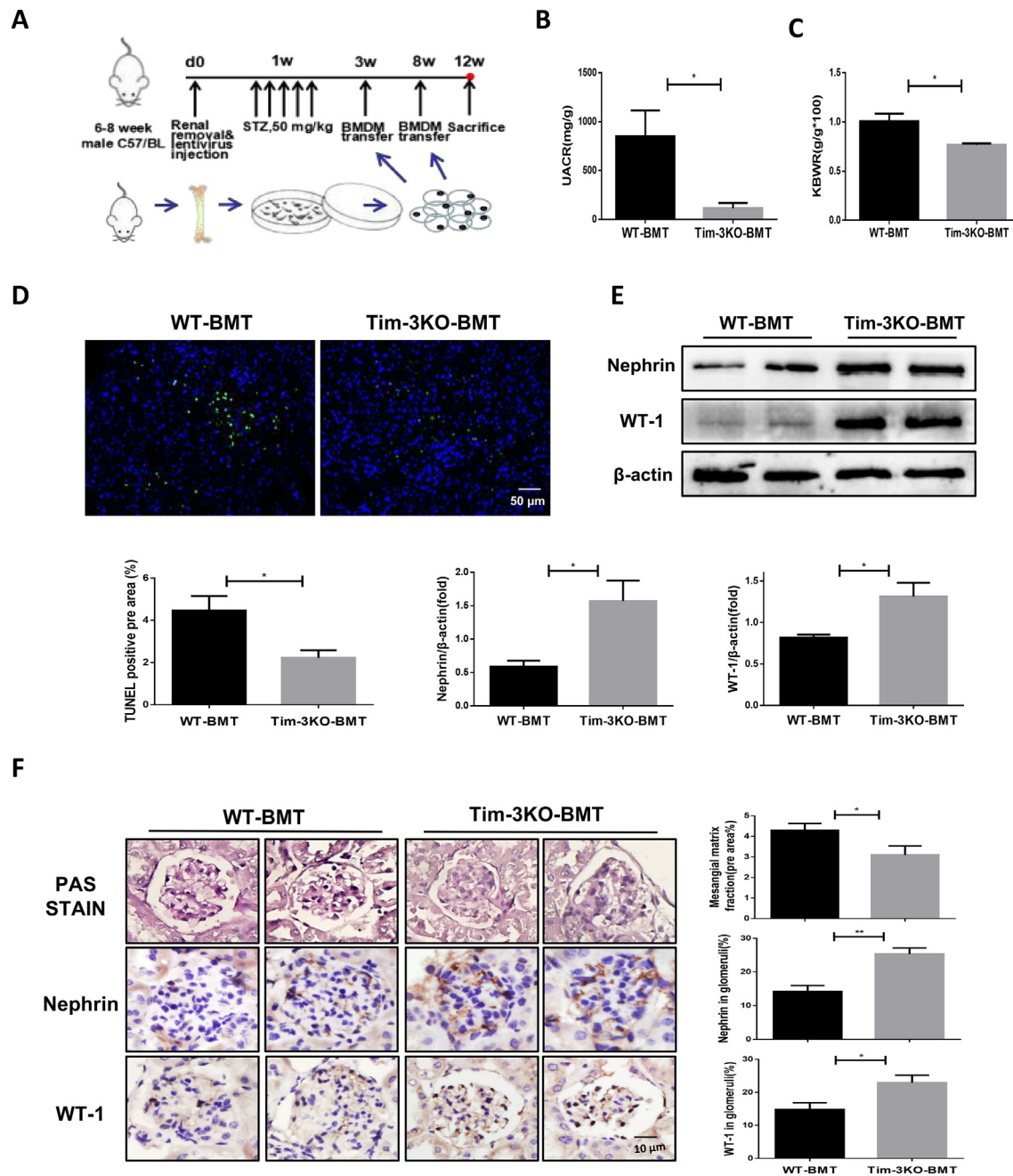
Figure 4: Adoptive transfer of Tim-3-positive macrophages aggravated podocyte dysfunction. (A) Experimental design for the BMT of diabetic mice. Transferred Tim-3-positive or deficient BMs back to Tim-3 KD mice. (B—C) UACR and KBWR in each group at 12 weeks of age after STZ injection. (D) Representative photomicrographs and quantifications of TUNEL staining for apoptotic renal cells in BMT mice. Bars = 50 μm. (E) Western blot analysis showing the relative protein levels of Nephrin and WT-1 in renal tissue of BMT mice. (F) Representative photomicrographs and quantifications of PAS staining and IHC staining of Nephrin and WT-1 in renal tissue in the different groups. Bars = 10 μm *P < 0.05, **P < 0.01 between such two BMT groups. BMT, bone marrow derived macrophage transfer.

podocytes, which is one of the key elements in renal damage of DN [36]. As shown in scratch assay, podocytes treated with CM from Tim-3 deficient macrophages migrated faster than that of WT macrophages (Figure 5E). CM from Tim-3-deficient macrophages also increased the numbers of migrated podocytes crossing the membrane over 12 h in a co-culture transwell system (Figure 5F). Taken together, these results support a critical role for Tim-3 expressing macrophages in podocyte disabilities such as aggravated foot process effacement, rearranged podocyte cytoskeleton and reduced cell motility.

3.5. Tim-3 exacerbates podocyte injury in a manner dependent on the NF-κB/TNF-α pathway

Activation NF-κB signaling ultimately results in macrophage activation, which is the key process of podocyte injury [4,37]. We therefore came to evaluate the involvement of NF-κB signaling in Tim-3-mediated renal damage. As expected, western blot analysis showed that phosphorylation of p65 was enhanced in kidney tissue from DN mice and was suppressed in renal tissue of diabetic Tim-3 KD mice (Figure 6A). This was further confirmed by IHC staining. As shown in
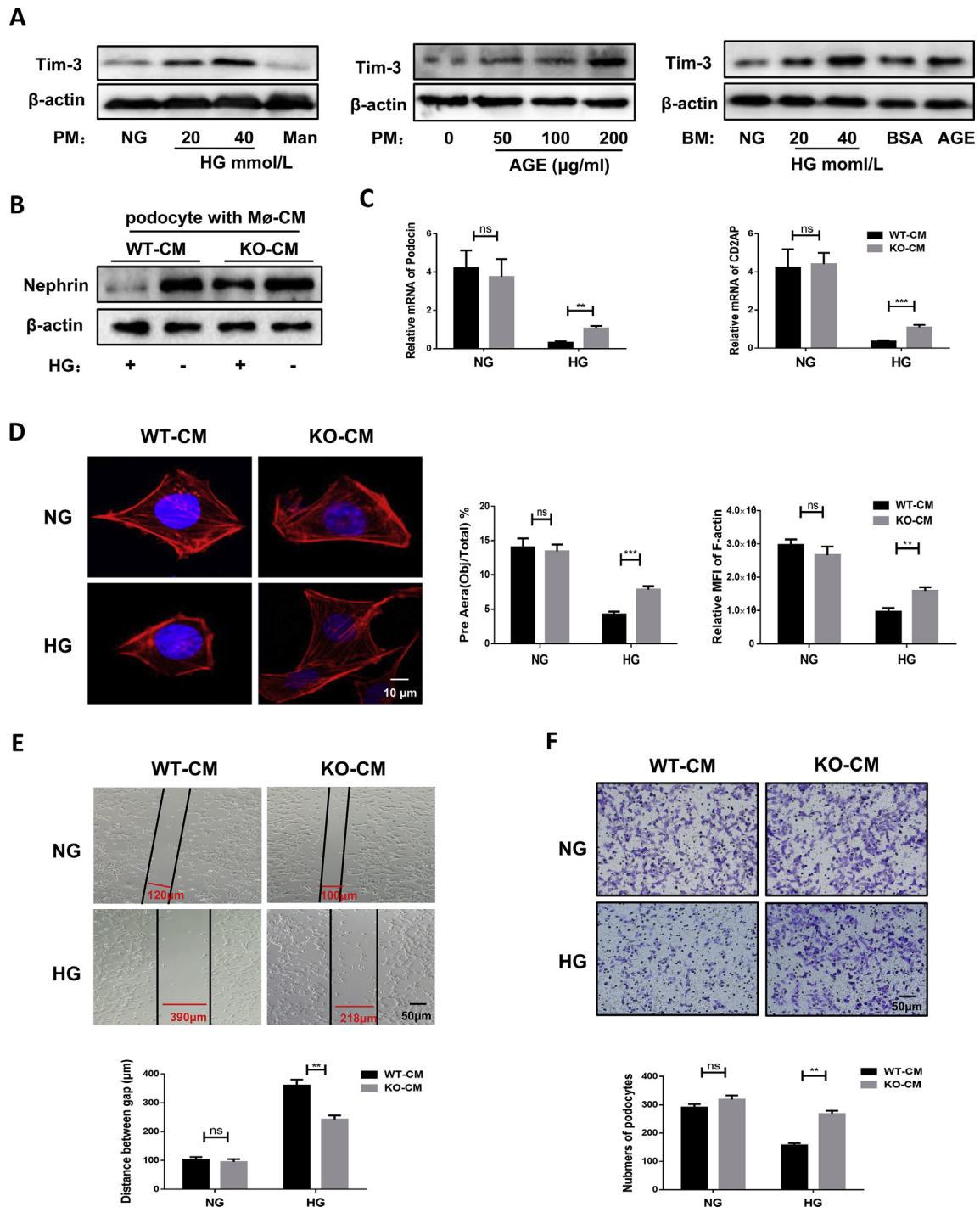
Figure 5: Enhanced Tim-3 expression in macrophage leading to severe podocyte injury with HG treatment. (A) Western blot analysis showing the relative protein level of Tim-3 treated with various stimulants in PMs and BMs. (B—E) Macrophage from either WT mice or Tim-3 KO mice were cultured with HG or NG medium and the culture medium was collected as macrophages conditioned medium (CM). Mouse podocyte (MPC) were stimulated with macrophage CM. Western blot (B) and RT-PCR (C) analysis showing the relative protein level of Nephrin and the relative mRNA levels of Podocin and CD2AP genes expressions. The podocyte cytoskeleton and its migration ability were assessed by immunofluorescence confocal (D), scratch assay (E) and transwell assay (F). $*P < 0.05$, $**P < 0.01$, $***P < 0.001$ vs normal glucose (n = 3). Data are expressed as means ± SEM, Student's t-test was employed for comparisons between two groups. PM, Peritoneal macrophage, BM, bone marrow-derived macrophage, HG, high glucose medium (20 and 40 mmol/L), AGE, advanced glycation end product (50, 100, 200 μg/ml), NG, normal glucose (11 mmol/L), MA, mannitol (40 mmol/L), BSA, bovine serum albumin (200 μg/ml).

Figure 6B, although STZ enhanced phosphorylation of p65 NF-κB in renal cortex and medulla, p-p65 was reduced in diabetic Tim-3 KD mice. Tim-3-mediated activation of p-p65 NF-κB in renal tissue was also detected in STZ treated WT and Tim-3 KO mice (Supplementary Fig. S6A, B). Interestingly, as downstream molecules, TNF-α but not IL-6 displayed similar expression pattern as p-p65 in renal tissue from diabetic Tim-3 KD mice (Figure 6C,D). In agreement, HG treatment significantly increased p-p65 in PMs from WT mice, but this
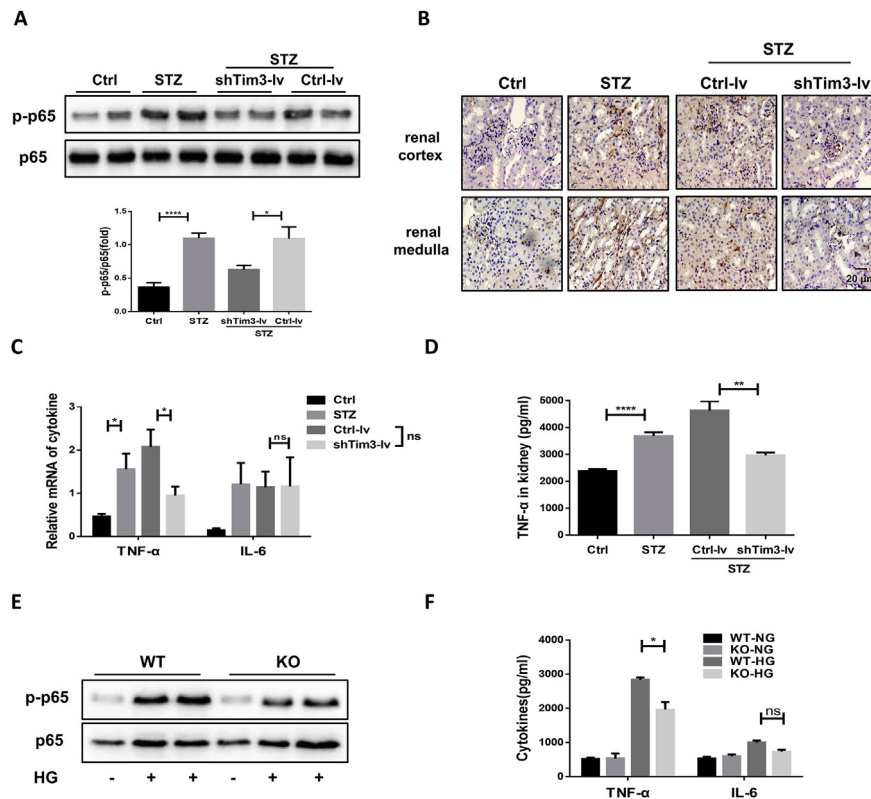
Figure 6: Down-regulation of Tim-3 suppressed the NF-κB/TNF-α signaling pathway in macrophages. (A) Western blot analysis showing the relative protein levels of phosph-p65 and total p65 in renal tissue of the different groups. (B) Representative photomicrographs of phosph-p65 IHC staining in renal glomeruli and tubulointerstitial region of different diabetic groups. Bars = 20 μm. (C) RT-PCR analysis showing the relative mRNA levels of TNF-α and IL-6 in renal tissue of of different groups. (D) Elisa analysis showing the excretion of TNF-α in renal tissue homogenate. (E) Western blot analysis showing the relative protein levels of phosph-p65 and total p65 in PMs stimulated with NG and HG medium. (F) Elisa analysis showing the relative mRNA levels of TNF-α and IL-6 in PMs treated with NG or HG. $*P < 0.05$, $**P < 0.01$, $***P < 0.001$, $****P < 0.0001$. Data are expressed as means ± SEM. One-way ANOVA followed by Tukey's post-test for multiple comparisons was used for groups of three or more.

enhancement was greatly suppressed in Tim-3 KO mice (Figure 6E). In Supplementary Fig. S6C, NF-κB phosphorylation especially adhered to Tim-3 positive macrophages in renal tissue, down-regulated Tim-3 expression in kidneys could decrease the NF-κB activation. The co-localization of Tim-3 and phosphate NF-κB also could be seen in renal samples of DN patients (Supplementary Fig. S2B). Also, PMs from Tim-3 KO mice produced significantly less TNF-α but not IL-6 in response to HG treatment compared with the WT control (Figure 6F). To explore whether the NF-κB signaling pathway involved in podocytes injury primed by Tim-3 expressing macrophages, MPC were stimulated with CM from NG/HG cultured macrophages pretreated with Tim-3-siRNA and NF-κB inhibitor (BAY11-7082). The NF-κB signaling pathway was successfully inhibited by pretreatment with BAY11-7082 at 10 μM for one hour (Supplementary Fig. S7A), and Tim-3 was also successfully down-regulated by Tim-3-siRNA transfection (Supplementary Fig. S7B). As shown in Figure 7A,C, BAY11-7082 not only greatly reversed the HG-treated macrophages mediated podocytes damage but also completely destroyed protective effects of Tim-3-deficient macrophages on podocyte damage, displaying as revised expression of Nephrin (Figure 7A) and re-arrangement of cytoskeleton (Figure 7C). TNF-α is the downstream of NF-κB, and it is mostly synthesized and released by infiltrating macrophages in the kidney treated with HG and AGE, causing damage to the glomerular permeability barrier [38,39]. In accordance with phosphorylation of p65 NF-κB, TNF-α excretion was decreased along with the NF-κB suppression by Tim-3 inhibition (Supplementary Fig. S7C). To characterize the potential role of TNF-α, PMs from TNF-α heterozygote (TNF-α$^{+/-}$)

mice or WT mice were transfected with Tim-3-siRNA and stimulated by NG and HG. TNF-α-depletion in macrophages was validated by RT-PCR (Supplementary Fig. S7D). As shown in Figure 7B,D, MPC treated with HG-CM from either TNF-α deficient or Tim-3 knockdown macrophages significantly inhibited the loss of Nephrin (Figure 7B) and the cytoskeleton derangement (Figure 7D). Overall, Tim-3 is essential for the activation of macrophages, leading to the phosphorylation of NF-κB and promoted TNF-α excretion in renal macrophages which in turn promotes podocyte foot process effacement and actin rearrangement, resulting in podocyte injury and proteinuria of DN.

4. DISCUSSION

Accumulated evidence demonstrates that Tim-3 exhibits diverse expressions and functions in different diseases [40,41]. However, the effects of Tim-3 in the progression of DN are still completely unknown. Recent evidence indicates that innate immunity rather than adaptive immunity is the major player in diabetic kidney [42], in which macrophages are the main components of renal immunity. In this study, for the first time, we identified upregulation of Tim-3 in diabetic renal macrophages. The genetic ablation of Tim-3 on macrophages ameliorated podocyte injury and foot process effacement in DN mice. Our data provides a novel mechanism for diabetic renal injury and suggests that targeting Tim-3 could be an attractive target for immunotherapy of DN.

Recently Tim-3 becomes a new hotspot in renal diseases. Increased Tim-3 expression has been reported in some non-neoplastic kidney
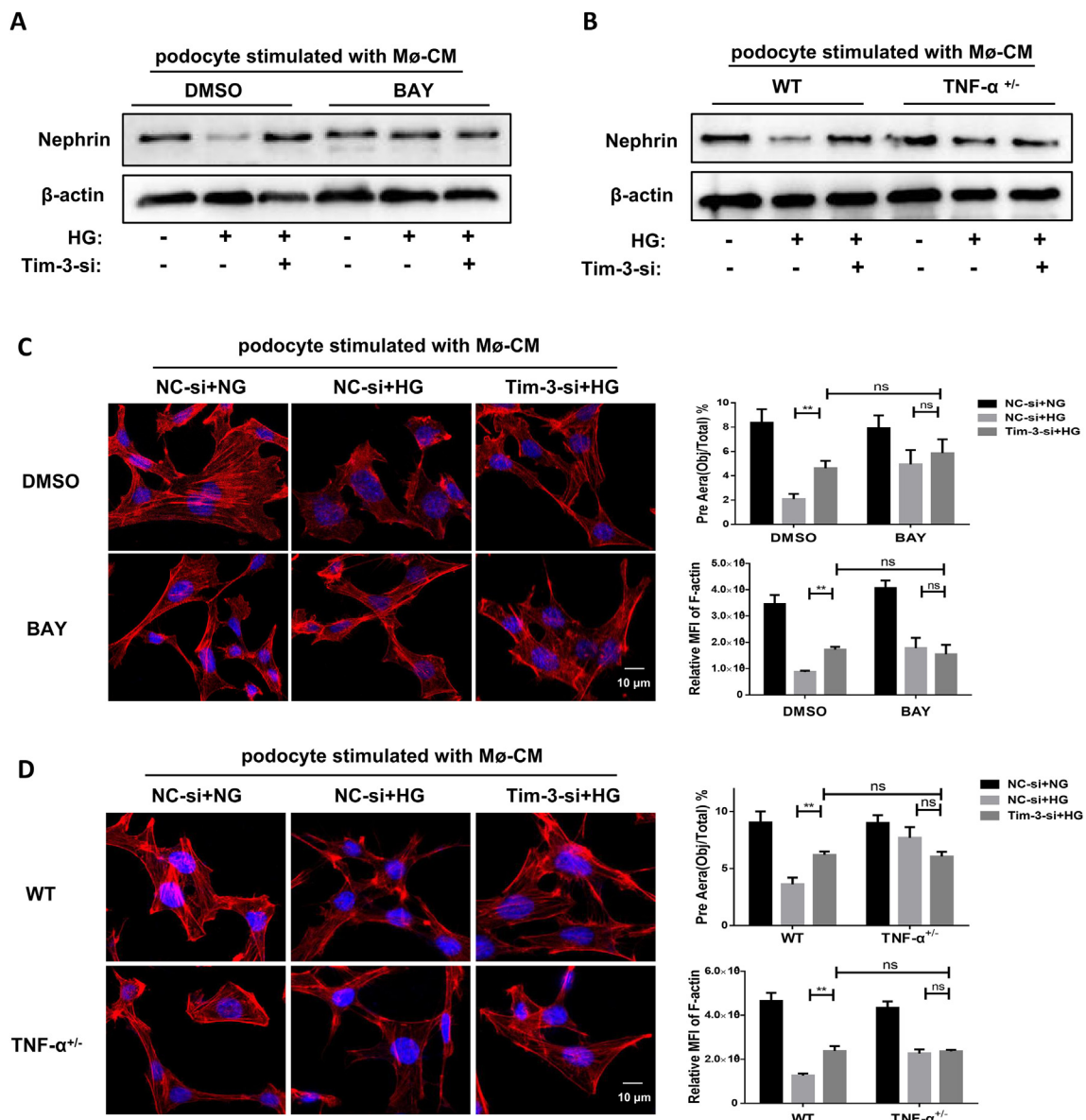
Figure 7: Tim-3 accelerated podocyte injury depending on the NF-κB/TNF-α signaling pathway in macrophages. MPC were stimulated with different CM from PMs in the following experiments. (A—B) Western blot analysis showing the relative protein level of Nephrin in podocytes stimulated with different CM. (C—D) Confocal microscopy analysis showing the expression and quantification of actin cytoskeleton stimulated with different CM. *P < 0.05, **P < 0.01 vs controls. Data are expressed as means ± SEM, Student's t-test was employed for comparisons between two groups; one-way ANOVA followed by Tukey's post-test for multiple comparisons was used for groups of three or more.

diseases which showed positive correlation with the pathological and serological index of patients from CKD like immunoglobulin A nephropathy (IgAN) and lupus nephritis (LN) [43,44], but the effects of Tim-3 in DN, the most common secondary chronic kidney disease in the clinic, and one of the leading causes of ESRD, are still unclear. In this study, with following evidence, we demonstrated that augmented Tim-3 expression in renal macrophages enhanced renal damages in DN. First, Tim-3 expression was significantly increased in diabetic kidney, especially on the surface of renal macrophages infiltrated in glomeruli and tubular interstitium, and the increased Tim-3 expression was associated with high level of proteinuria (Figure 1). Second, eliminated renal damage was not only detected in STZ-DN mice treated with Tim-3 shRNA-expressing lentivirus but also displayed in global Tim-3 KO DN mice (Figure 3). Third, transfer of Tim-3-expressing macrophages enhanced renal injury of DN mice with

Tim-3-knockdown (Figure 4). More importantly, clinical study showed that abundant Tim-3 expression in human renal samples had a positive correlation with poor renal function of diabetic patients (Figure 2), further supporting that Tim-3 on macrophages plays critical roles in renal damage in DN. Direct evidence of the interaction between Tim-3 mediated macrophage activation and podocyte damage came from *in vitro* studies with podocyte cultures under treatment with conditioned medium (CM) collected from NG/HG containing medium-stimulated macrophages with or without Tim-3 (Figure 5). Although mounting evidence indicates that HG and AGE trigger the structural and functional changes of glomerular basement membrane (GBM) and damage the neighbor cells [34,45,46], cell—cell interactions between macrophages and podocytes have not been described comprehensively in DN. Our *in vitro* data here showed that podocytes suffered much more damage from Tim-3 abundant macrophages with HG-CM

treatment rather than Tim-3 KO macrophages (Figure 5), strongly suggesting that Tim-3 aggravated diabetic renal injury through regulating macrophage activation.

The other important question we focused on is how augmented Tim-3 on macrophages induced podocyte injury under HG stimulation. Studies have shown that multiple signaling pathways are involved in DN, in which NF-κB is the most common transcription factor contributes to the incidence of chronic inflammation and renal dysfunction [37,47]. Activation of NF-κB signaling pathway in macrophages upregulates production of cytokines and chemokines in renal tissue, leading to the recruitment and activation of other cells, eventually causes renal damage [10,48]. Although in 2013, Yang et al. showed that Tim-3 signaling increased the LPS-induced phosphorylation of PI3K-AKT and inhibited NF-κB activation in macrophages [23], controversial results had been noted in EAE with Tim-3 activating NF-κB in macrophages and resulting in tissue damage [15]. Therefore, the interaction between Tim-3 and NF-κB signaling might be disease dependent. Here, our results demonstrated that NF-κB was widely expressed in the renal macrophages of DN, and Tim-3 knockout inhibited the phosphorylation of p65 in HG treated macrophages (Figure 6), which is consistent with the effect of Tim-3 in EAE mice [15]. Moreover, NF-κB inhibitor largely abrogated the protective effect of Tim-3-knockout on macrophages, resulting in equal podocyte damage under macrophage CM stimulation. Therefore, Tim-3-mediated macrophage activation in DN at least partly relies on NF-κB signaling pathway.

Downstream of NF-κB, early release of IL-1, IL-6, and TNF-α associated with overwhelming innate inflammatory responses are of great importance to DN [49]. Our previous study showed that Tim-3 activated NF-κB signaling pathway and induced secretion of IL-6 in tumor-associated macrophages (TAMs) infiltrated in hepatocellular carcinoma (HCC) [24]. However, in this study, we did not detect significant difference of IL-6 production under the interference of Tim-3 in DN mice (Figure 6). Alternatively, silencing Tim-3 either in kidney tissue or in macrophages led to renal protection by reduction of TNF-α (Figure 6), suggesting TNF-α as the downstream molecule of NF-κB signaling pathway regulated by Tim-3 in DN. This is consistent with the well described role of TNF-α as the primer inducer and driver of renal micro-inflammation, which plays a central role in the network of pro-inflammatory molecules during the progression of DN [50]. In agreement, further *in vitro* studies using TNF-α deficient macrophages showed that TNF-α deficiency abolished the podocyte damage mediated by macrophages with Tim-3-knockdown. Thus, Tim-3 promotes renal macrophage activation through NF-κB/TNF-α signaling pathway in DN. Detail mechanism underling the Tim-3 promoted NF-κB/TNF-α signaling needs further investigations which will be definitely benefit for immunotherapy of DN using Tim-3 as target.

Although here we mainly focus our work on the role of Tim-3 on macrophages promoted renal damage, so far, we cannot exclude the involvement of Tim-3 expressed on other immune cells and renal resident cells. In fact, we detected Tim-3 expressions on different subsets in both glomerular and tubular compartments of the kidney, except macrophages; NK cells from DN mice displayed much higher expression level of Tim-3 than that from control mice. Interestingly, Tim-3 was also partly expressed in both renal glomerular and tubular compartments of diabetic patients and animals. Further studies are still needed to reveal the functions and precise mechanisms of Tim-3 in DN both *in vitro* and *in vivo*.

In conclusion, our study for the first time demonstrates that the immune checkpoint molecule Tim-3 accelerates podocyte injury, which aggravates the progression of DN by triggering the NF-κB/TNF-α signaling pathway in macrophages. Hence, highlights the potential role of Tim-3 as a new target aiming at macrophages for the clinical application to DN.

CONFLICT OF INTEREST

The authors declare no competing of interests.

APPENDIX A. SUPPLEMENTARY DATA

Supplementary data to this article can be found online at https://doi.org/10.1016/j.molmet.2019.02.007.

REFERENCES

[1] Ma, R.C.W., 2018. Epidemiology of diabetes and diabetic complications in China. Diabetologia 61:1249—1260.

[2] Umanath, K., Lewis, J.B., 2018. Update on diabetic nephropathy: core curriculum 2018. American Journal of Kidney Diseases 71:884—895.

[3] Wang, L., Gao, P., Zhang, M., Huang, Z., Zhang, D., Deng, Q., et al., 2017. Prevalence and ethnic pattern of diabetes and prediabetes in China in 2013. JAMA 317:2515—2523.

[4] Hickey, F.B., Martin, F., 2018. Role of the immune system in diabetic kidney disease. Current Diabetes Reports 18:20.

[5] Tesch, G.H., 2017. Diabetic nephropathy - is this an immune disorder? Clinical Science 131:2183—2199.

[6] Sassy-Prigent, C., Heudes, D., Mandet, C., Bélair, M.F., Michel, O., Perdereau, B., et al., 2000. Early glomerular macrophage recruitment in streptozotocin-induced diabetic rats. Diabetes 49:466—475.

[7] Chow, F., Ozols, E., Nikolic-Paterson, D.J., Atkins, R.C., Tesch, G.H., 2004. Macrophages in mouse type 2 diabetic nephropathy: correlation with diabetic state and progressive renal injury. Kidney International 65:116—128.

[8] You, H., Gao, T., Cooper, T.K., Brian Reeves, W., Awad, A.S., 2013. Macrophages directly mediate diabetic renal injury. American Journal of Physiology Renal Physiology 305:F1719—F1727.

[9] de Zeeuw, D., Bekker, P., Henkel, E., Hasslacher, C., Gouni-Berthold, I., Mehling, H., et al., 2015. The effect of CCR2 inhibitor CCX140-B on residual albuminuria in patients with type 2 diabetes and nephropathy: a randomised trial. Lancet Diabetes Endocrinol 3:687—696.

[10] Caamano, J., Hunter, C.A., 2002. NF- B family of transcription factors: central regulators of innate and adaptive immune functions. Clinical Microbiology Reviews 15:414—429.

[11] Kuhad, A., Chopra, K., 2009. Attenuation of diabetic nephropathy by tocotrienol: involvement of NFkB signaling pathway. Life Sciences 84:296—301.

[12] Zhang, Z., Yuan, W., Sun, L., Szeto, F.L., Wong, K.E., Li, X., et al., 2007. 1,25-Dihydroxyvitamin D3 targeting of NF-kappaB suppresses high glucose-induced MCP-1 expression in mesangial cells. Kidney International 72:193—201.

[13] Liu, Z., Han, Y., Zhao, F., Zhao, Z., Tian, J., Jia, K., 2018. Nobiletin suppresses high-glucose-induced inflammation and ECM accumulation in human mesangial cells through STAT3/NF-kappaB pathway. Journal of Cellular Biochemistry.

[14] Sabatos, C.A., Chakravarti, S., Cha, E., Schubart, A., Sanchez-Fueyo, A., Zheng, X.X., et al., 2003. Interaction of Tim-3 and Tim-3 ligand regulates T helper type 1 responses and induction of peripheral tolerance. Nature Immunology 4:1102—1110.

[15] Anderson, A.C., Anderson, D.E., Bregoli, L., Hastings, W.D., Kassam, N., Lei, C., et al., 2007. Promotion of tissue inflammation by the immune receptor Tim-3 expressed on innate immune cells. Science 318:1141—1143.

[16] Han, G., Chen, G., Shen, B., Li, Y., 2013. Tim-3: an activation marker and activation limiter of innate immune cells. Frontiers in Immunology 4:449.

[17] Ocana-Guzman, R., Torre-Bouscoulet, L., Sada-Ovalle, I., 2016. TIM-3 regulates distinct functions in macrophages. Frontiers in Immunology 7:229.

[18] Yu, A., Zhang, X., Li, M., Ye, P., Duan, H., Zhang, T., et al., 2017. Tim-3 enhances brain inflammation by promoting M1 macrophage polarization following intracerebral hemorrhage in mice. International Immunopharmacology 53:143—148.

[19] Sun, J., Huang, Q., Li, S., Meng, F., Li, X., Gong, X., 2018. miR-330-5p/Tim-3 axis regulates macrophage M2 polarization and insulin resistance in diabetes mice. Molecular Immunology 95:107—113.

[20] Jiang, X., Yu, J., Shi, Q., Xiao, Y., Wang, W., Chen, G., et al., 2015. Tim-3 promotes intestinal homeostasis in DSS colitis by inhibiting M1 polarization of macrophages. Clinical Immunology 160:328—335.

[21] Koh, H.S., Chang, C.Y., Jeon, S.B., Yoon, H.J., Ahn, Y.H., Kim, H.S., et al., 2015. The HIF-1/glial TIM-3 axis controls inflammation-associated brain damage under hypoxia. Nature Communications 6:6340.

[22] Du, X., Wu, Z., Xu, Y., Liu, Y., Liu, W., Wang, T., et al., 2018. Increased Tim-3 expression alleviates liver injury by regulating macrophage activation in MCD-induced NASH mice. Cellular and Molecular Immunology.

[23] Yang, X., Jiang, X., Chen, G., Xiao, Y., Geng, S., Kang, C., et al., 2013. T cell Ig mucin-3 promotes homeostasis of sepsis by negatively regulating the TLR response. The Journal of Immunology 190:2068—2079.

[24] Yan, W., Liu, X., Ma, H., Zhang, H., Song, X., Gao, L., et al., 2015. Tim-3 fosters HCC development by enhancing TGF-β-mediated alternative activation of macrophages. Gut 64:1593—1604.

[25] Guo, Y., Zhang, J., Lai, X., Chen, M., Guo, Y., 2018. Tim-3 exacerbates kidney ischaemia/reperfusion injury through the TLR-4/NF-kappaB signalling pathway and an NLR-C4 inflammasome activation. Clinical and Experimental Immunology 193:113—129.

[26] Zhang, H., Song, Y., Yang, H., Liu, Z., Gao, L., Liang, X., et al., 2018. Tumor cell-intrinsic Tim-3 promotes liver cancer via NF-kappaB/IL-6/STAT3 axis. Oncogene 37:2456—2468.

[27] Wang, X., Liu, J., Zhen, J., Zhang, C., Wan, Q., Liu, G., et al., 2014. Histone deacetylase 4 selectively contributes to podocyte injury in diabetic nephropathy. Kidney International 86:712—725.

[28] Liu, M., Liang, K., Zhen, J., Zhou, M., Wang, X., Wang, Z., et al., 2017. Sirt6 deficiency exacerbates podocyte injury and proteinuria through targeting Notch signaling. Nature Communications 8:413.

[29] Zhang, S., Zhang, Y., Wei, X., Zhen, J., Wang, Z., Li, M., et al., 2010. Expression and regulation of a novel identified TNFAIP8 family is associated with diabetic nephropathy. Biochimica et Biophysica Acta 1802:1078—1086.

[30] Kawakami, T., Lichtnekert, J., Thompson, L.J., Karna, P., Bouabe, H., Hohl, T.M., et al., 2013. Resident renal mononuclear phagocytes comprise five discrete populations with distinct phenotypes and functions. The Journal of Immunology 191:3358—3372.

[31] Ikezumi, Y., Hurst, L.A., Masaki, T., Atkins, R.C., Nikolic-Paterson, D.J., 2003. Adoptive transfer studies demonstrate that macrophages can induce proteinuria and mesangial cell proliferation. Kidney International 63:83—95.

[32] Liu, J., Li, Q.X., Wang, X.J., Zhang, C., Duan, Y.Q., Wang, Z.Y., et al., 2016. beta-Arrestins promote podocyte injury by inhibition of autophagy in diabetic nephropathy. Cell Death & Disease 7:e2183.

[33] Tent, H., Sanders, J.S., Rook, M., Hofker, H.S., Ploeg, R.J., Navis, G., et al., 2012. Effects of preexistent hypertension on blood pressure and residual renal function after donor nephrectomy. Transplantation 93:412—417.

[34] Lin, J.S., Susztak, K., 2016. Podocytes: the weakest link in diabetic kidney disease? Current Diabetes Reports 16:45.

[35] Guo, Y., Song, Z., Zhou, M., Yang, Y., Zhao, Y., Liu, B., et al., 2017. Infiltrating macrophages in diabetic nephropathy promote podocytes apoptosis via TNF-alpha-ROS-p38MAPK pathway. Oncotarget 8:53276—53287.

[36] Sever, S., Schiffer, M., 2018. Actin dynamics at focal adhesions: a common endpoint and putative therapeutic target for proteinuric kidney diseases. Kidney International 93:1298—1307.

[37] Mezzano, S., Aros, C., Droguett, A., Burgos, M.E., Ardiles, L., Flores, C., et al., 2004. NF-kappaB activation and overexpression of regulated genes in human diabetic nephropathy. Nephrology Dialysis Transplantation 19:2505—2512.

[38] Navarro, J.F., Mora-Fernandez, C., 2006. The role of TNF-alpha in diabetic nephropathy: pathogenic and therapeutic implications. Cytokine & Growth Factor Reviews 17:441—450.

[39] Awad, A.S., You, H., Gao, T., Cooper, T.K., Nedospasov, S.A., Vacher, J., et al., 2015. Macrophage-derived tumor necrosis factor-alpha mediates diabetic renal injury. Kidney International 88:722—733.

[40] Das, M., Zhu, C., Kuchroo, V.K., 2017. Tim-3 and its role in regulating anti-tumor immunity. Immunological Reviews 276:97—111.

[41] Anderson, A.C., Anderson, D.E., 2006. TIM-3 in autoimmunity. Current Opinion in Immunology 18:665—669.

[42] Wada, J., Makino, H., 2016. Innate immunity in diabetes and diabetic nephropathy. Nature Reviews Nephrology 12:13—26.

[43] Yang, X., Hu, Z., Xia, X., Zhen, J., Zhuang, X., Peng, T., 2014. Expression of human T cell immunoglobulin domain and mucin-3 on kidney tissue from immunoglobulin A nephropathy patients. Immunologic Research 60:85—90.

[44] Guo, L., Yang, X., Xia, Q., Zhen, J., Zhuang, X., Peng, T., 2014. Expression of human T cell immunoglobulin domain and mucin-3 (TIM-3) on kidney tissue from systemic lupus erythematosus (SLE) patients. Clinical and Experimental Medicine 14:383—388.

[45] Forbes, J.M., Cooper, M.E., 2013. Mechanisms of diabetic complications. Physiological Reviews 93:137—188.

[46] Pavenstadt, H., Kriz, W., Kretzler, M., 2003. Cell biology of the glomerular podocyte. Physiological Reviews 83:253—307.

[47] Rangan, G., Wang, Y., Fau-Harris, D., Harris, D., 2009. NF-kappaB signalling in chronic kidney disease. Frontiers in Bioscience 14:3496—3552.

[48] Li, Q., Verma, I.M., 2002. NF-kappaB regulation in the immune system. Nature Reviews Immunology 2:725—734.

[49] Cao, S., Zhang, X., Edwards, J.P., Mosser, D.M., 2006. NF-kappaB1 (p50) homodimers differentially regulate pro- and anti-inflammatory cytokines in macrophages. Journal of Biological Chemistry 281:26041—26050.

[50] Sun, L., Kanwar, Y.S., 2015. Relevance of TNF-alpha in the context of other inflammatory cytokines in the progression of diabetic nephropathy. Kidney International 88:662—665.